Int. J. Electron. Commun. (AEÜ) 64 (2010) 1137–1147

Contents lists available at ScienceDirect

Int. J. Electron. Commun. (AEÜ)

journal homepage: www.elsevier.de/aeue

A novel statistical image thresholding method

Zuoyong Li [a,b,*], Chuancai Liu [a], Guanghai Liu [c], Yong Cheng [a], Xibei Yang [a], Cairong Zhao [a,b]

[a] School of Computer Science and Technology, Nanjing University of Science and Technology, Nanjing 210094, China
[b] Department of Computer Science, Minjiang University, Fuzhou 350108, China
[c] School of Computer Science and Information Technology, Guangxi Normal University, Guilin 541004, China

ARTICLE INFO

Article history:
Received 3 April 2009
Accepted 27 October 2009

Keywords:
Thresholding
Image segmentation
Variance
Standard deviation
Statistical theory

ABSTRACT

Classic statistical thresholding methods based on maximizing between-class variance and minimizing class variance fail to achieve satisfactory results when segmenting a kind of image, where variance discrepancy between the object and background classes is large. The reason is that they take only class variance sum of some form as criterions for threshold selection, but neglect discrepancy of the variances. In this paper, a novel criterion combining the above two factors is proposed to eliminate the described limitation for classic statistical approaches and improve segmentation performance. The proposed method determines the optimal threshold by minimizing the criterion. The method was compared with several classic thresholding methods on a variety of images including some NDT images and laser cladding images, and the experimental results show the effectiveness of the algorithm.

1. Introduction

Image segmentation is a critical preprocess step in image analysis and pattern recognition [1–4]. Thresholding is one of the most important and effective techniques, and plays a key role when segmenting images with distinctive gray levels corresponding to object and background. Its aim is to find an appropriate threshold for separating the object from the background. Thresholded result is a binary image where all pixels with gray levels higher than the determined threshold are classified as object and the rest of pixels are assigned to background, or vice versa. The technique can serve a variety of applications, such as biomedical image analysis [5], handwritten character identification [6], automatic target recognition [7] and change detection [8].

Thresholding methods can be classified into parametric and nonparametric approaches [9–17]. The former assumes gray level distribution of each class obey a given distribution, usually a normal distribution, and finds the optimal threshold by estimating the parameters of the distribution using the given histogram. This typically leads to a nonlinear estimation problem of expensive computation. The latter usually determines the optimal threshold by optimizing certain objective function, such as between-class variance [11], variance [13], entropy [14–16] and energy [17]. The nonparametric approach is proved to be more robust and accurate than the parametric one.

Many thresholding approaches have been developed over the past years. For example, Tsai's parametric method [9] finds the optimal threshold on the condition that the thresholded image has the same moment as the original one. Bazi et al. [10] proposed a parametric and global method, which assumes that the object and background classes follow a generalized Gaussian distribution, and finds the threshold from the estimation of the parameters of the two classes by the expectation maximization algorithm. Otsu's method [11] chooses the optimal threshold by maximizing the between-class variance of gray levels in the object and background portions. Sahoo et al. [12] found that Otsu's method was one of the better threshold selection approaches for general real world images with regard to uniformity and shape measures. Hou et al. [13] presented an approach based on minimizing class variance, which can be regarded as a generalization of Otsu's, where the term of class variance follows the precise definition of variance for a class. In Pun's method [14], the optimal threshold is determined by maximizing a posteriori entropy of the object and background portions. Kapur et al. [15] found some flaws in Pun's derivations and presented a corrected entropy-based method. Kittler and Illingworth [18] suggested a method, which approximates the histogram by a mixture of normal distributions and minimizes the classification error probability. A thorough survey over thresholding techniques is provided in the literature [19].

Among these methods, statistical thresholding approaches are popular for the simplicity and efficiency. Otsu's [11] and Hou's methods [13] are two typical examples. The former tends to dichotomize an image into object and background of similar sizes. After exploring the underlying mechanism responsible for Otsu's bias, Hou presented a generalized Otsu's method. Unfortunately,

* Corresponding author at: School of Computer Science and Technology, Nanjing University of Science and Technology, Nanjing 210094, China. Tel.: +86 15950568429; fax: +86 02584315751.
E-mail addresses: fzulzytdq@126.com, fzulzytdq@yahoo.com.cn (Z. Li).

1434-8411/$ - see front matter © 2009 Elsevier GmbH. All rights reserved.
doi:10.1016/j.aeue.2009.11.011

both methods subject to a limitation of being unable to obtain satisfactory results when segmenting some images of large variance discrepancy in the object and background classes. The reason is that the two approaches take only class variance sum of some form into account, but neglect discrepancy of class variances. As an attempt to eliminate the limitation of Otsu's and Hou's methods, a new statistical thresholding method is presented in this paper. The proposed method takes class variance sum and variance discrepancy into account at the same time and constructs a novel statistical criterion for threshold selection. The performance of the proposed method is compared with four classic thresholding methods by testing a variety of real world images. Experimental results show its superiority over its counterparts.

The remainder of this paper is organized as follows: Section 2 introduces two classic statistical methods and the proposed criterion. The performance of the proposed method is tested on a variety of images and is compared with other methods in Section 3. Conclusions appear in Section 4.

2. Thresholding algorithm

In this section, two classic thresholding methods, i.e., Otsu's and Hou's methods, are first briefly reviewed, and their respective limitation for image segmentation is also discussed. A new thresholding criterion and the corresponding algorithm are then proposed to eliminate this limitation.

2.1. Classic statistical methods

Without losing generality, let I denote a gray scale image with L gray levels $[0,1,\ldots,L-1]$. The number of pixels with gray level i is denoted by n_i and the total number of pixels by $N=n_0+n_1+\cdots+n_{L-1}$. The probability of gray level i appeared in the image is defined as

$$p_i=\frac{n_i}{N},\quad p_i\geq 0,\quad \sum_{i=0}^{L-1}p_i=1. \tag{1}$$

Suppose that the pixels in the image are divided into two classes C_1 and C_2 by a gray level t; C_1 is the set of pixels with levels $[0,1,\ldots,t]$, and the rest of pixels belong to C_2. C_1 and C_2 normally correspond to the object class and the background one, or vice versa. Then the probabilities of the two classes are given by

$$\omega_1=\sum_{i=0}^{t}p_i, \tag{2}$$

$$\omega_2=\sum_{i=t+1}^{L-1}p_i. \tag{3}$$

The mean gray levels of the two classes can be defined as

$$\mu_1=\sum_{i=0}^{t}ip_i/\omega_1, \tag{4}$$

$$\mu_2=\sum_{i=t+1}^{L-1}ip_i/\omega_2, \tag{5}$$

and corresponding class variances are given by

$$\sigma_1^2=\sum_{i=0}^{t}(i-\mu_1)^2p_i/\omega_1, \tag{6}$$

$$\sigma_2^2=\sum_{i=t+1}^{L-1}(i-\mu_2)^2p_i/\omega_2. \tag{7}$$

The within-class variance, the between-class variance and the total variance of gray levels in Otsu's method [11] can be defined by

$$\sigma_W^2=\omega_1\sigma_1^2+\omega_2\sigma_2^2, \tag{8}$$

$$\sigma_B^2=\omega_1\omega_2(\mu_2-\mu_1)^2, \tag{9}$$

$$\sigma_T^2=\sum_{i=0}^{L-1}(i-\mu_T)^2p_i, \tag{10}$$

where

$$\mu_T=\sum_{i=0}^{L-1}ip_i. \tag{11}$$

According to the above equations, the following basic relation always holds:

$$\sigma_W^2+\sigma_B^2=\sigma_T^2. \tag{12}$$

Because σ_W^2 and σ_B^2 are functions of gray level t, while σ_T^2 is independent of t. Maximizing the between-class variance is equivalent to minimizing the within-class variance. Thus the optimal threshold t^* can be determined by Otsu's method,

$$t^*=\mathrm{Arg}\min_{0\leq t\leq L-1}\{\sigma_W^2(t)\}. \tag{13}$$

Otsu's method is regarded as one of the better threshold selection approaches for general real world images, but it has a weakness of tending to classify an image into two parts of similar sizes regardless of the practical size of object. After exploring the potential reason for Otsu's weakness, Hou et al. found a generalized version of Otsu's method to overcome it. Hou's method defines a new objective function, class variance sum of two thresholded classes, and finds the optimal threshold by minimizing the function. The optimal threshold t^* can be sought as follows:

$$t^*=\mathrm{Arg}\min_{0\leq t\leq L-1}\{\sigma_1^2(t)+\sigma_2^2(t)\}. \tag{14}$$

Otsu's and Hou's methods choose class variance sum of some form as criterions for threshold selection. Their difference is the parameters of two class variances.

2.2. New criterion

Unfortunately, the above statistical methods only consider class variance sum, but neglect variance discrepancy between foreground (object) and background. So they are not suitable for segmenting image of large class variance difference in the object and background. For example, the object has slight gray level changes and small class variance, while the background has big gray level changes and large class variance. This type of image mainly includes laser cladding images and some nondestructive testing (NDT) images. Fig. 1(a) gives an example, which is a thermal image of GFRP composite material. Its histogram of bimodal distribution with unequal sizes and ground truth image are shown in Figs. 1(b) and (c). Manual threshold corresponding to the ground truth image is 227, which locates at the valley of two peaks. Variances of the background and object classes in the thresholded result obtained by the manual threshold are 1325.979 and 11.62196, respectively, which shows large variance discrepancy. The explanation to this is that the object has slight gray level changes, while the background corresponds to sharp gray level changes as can be observed in Fig. 1(a). In this case, both Otsu's and Hou's methods give incorrect thresholds (i.e., 151 and 158) and fail to separate the object from the background as shown in Figs. 1(d) and (e). They tend to divide the

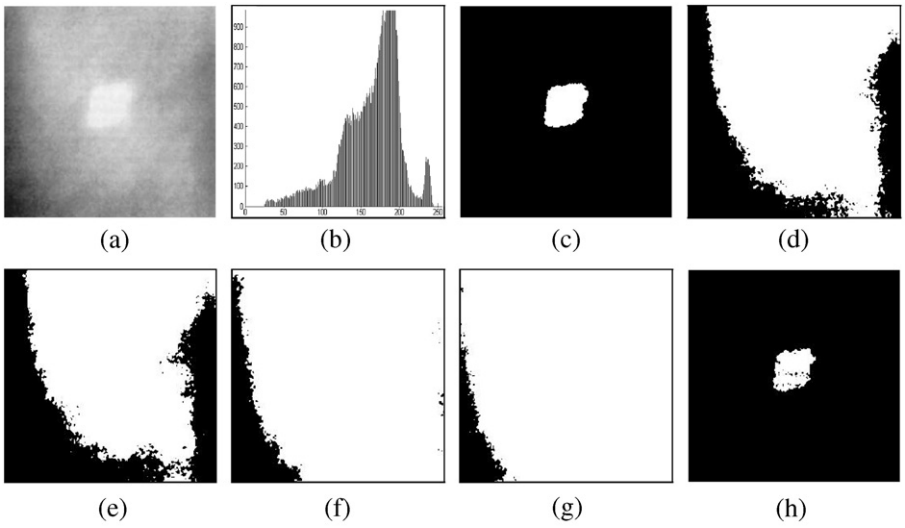

Fig. 1. Thresholding results of GFRP image: (a) original, (b) histogram, (c) ground truth image, (d) Otsu's method ($t = 151$), (e) Hou's method ($t = 158$), (f) KAPUR ($t = 118$), (g) MET ($t = 92$), (h) the proposed method with $\alpha = 0.5$ ($t = 232$).

Table 1
Thresholds, numbers of misclassified pixels, values of ME, FPR and FNR, and running times obtained by using different methods for the NDT images.

Images	Thresholding methods				
	Otsu's method	Hou's method	KAPUR	MET	The proposed method
GFRP					
Threshold	151	158	118	92	232
Misclassified pixels	42475	38821	56016	59409	347
ME	0.64812	0.59236	0.85474	0.90651	0.0052948
FPR	0.67079	0.61308	0.88464	0.93822	0
FNR	0	0	0	0	0.15666
Running time (s)	1.266	3.344	0.25	2.047	2.75
PCB					
Threshold	104	112	158	64	99
Misclassified pixels	530	1753	13576	5539	131
ME	0.0080872	0.026749	0.20715	0.084518	0.0019989
FPR	0	0	0	0.12542	0.0029661
FNR	0.0248	0.082027	0.63525	0	0
Running time (s)	0.235	2.781	0.047	0.406	3.047
Material					
Threshold	154	157	119	177	167
Misclassified pixels	6788	5343	22021	3275	1240
ME	0.10358	0.081528	0.33601	0.049973	0.018921
FPR	0.20864	0.16423	0.67686	0	0.038114
FNR	0	0	0	0.099236	0
Running time (s)	0.828	2.953	0.031	0.485	3.5

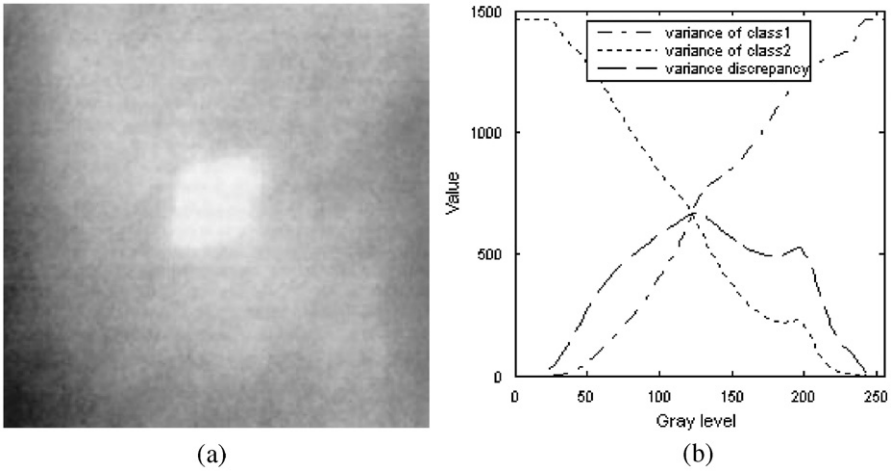

Fig. 2. Variances of GFRP image: (a) original, (b) variance discrepancy and variances of the object and background classes.

image into two components with similar sizes. Quantitative comparisons of segmentation results refer to Table 1.

In order to eliminate the above limitation of Otsu's and Hou's methods, a novel criterion combining class variance sum with variance discrepancy is proposed, which can be formulated as

$$J(\alpha,t)=\alpha(\sigma_1^2(t)+\sigma_2^2(t))+(1-\alpha)\sigma_D(t), \tag{15}$$

where

$$\sigma_D(t)=\sigma_1(t)\sigma_2(t), \tag{16}$$

and $\sigma_1^2(t)\le\sigma_D(t)\le\sigma_2^2(t)$ or $\sigma_2^2(t)\le\sigma_D(t)\le\sigma_1^2(t)$. $\sigma_D(t)$ is used to measure variance discrepancy of two thresholded classes, $\sigma_1(t)$ and $\sigma_2(t)$ are their respective standard deviation. It is worth mentioning that small $\sigma_D(t)$ usually corresponds to large variance discrepancy as illustrated in Fig. 2(b). This figure includes three curves, where class1 indicates the class with levels $[0,1,\ldots,t]$, class2 is for $[t+1,\ldots,L-1]$. The parameter α in Eq. (15) is a weight that balances contributions of variance sum and variance discrepancy. When $\alpha=1$, the new criterion degenerates to Hou's criterion. Thus the proposed method can be regarded as a generalized version of Hou's method.

The optimal threshold t^* can be determined by minimizing the new criterion

$$J(\alpha,t^*)=\mathrm{Arg}\min_{0\le t\le L-1}J(\alpha,t). \tag{17}$$

Eq. (17) actually attempts to decrease the effect of class variance sum and emphasize the influence of variance discrepancy simultaneously. In this way, the variance discrepancy becomes an explicit factor for determining the optimal threshold. Fig. 3 gives curves of Hou's criterion and the new one for the images used in our experiments. From the figure, one can see that: (1) the two curves are similar in shape, (2) in spite of the shape similarity, their respective lowest point usually positions at different location, that is, the thresholds determined by the two methods are different.

For the above image I with L gray levels, the process determining the optimal threshold t^* in our method is as follows:

(1) Initialize MJ to be infinite and $t=0$, where MJ is the minimum value of $J(\alpha,t)$, t is the temporal gray level.
(2) Repeat steps 3–4, L times.
(3) Compute the value of the criterion $J(\alpha,t)$ corresponding to gray level t by Eq. (15).
(4) Compare $J(\alpha,t)$ and MJ, if $J(\alpha,t)<MJ$, then $MJ=J(\alpha,t), t^*=t$ and $t=t+1$; else, $t=t+1$.

3. Experimental results

To evaluate the performance of the proposed method, a variety of real world images including those in nondestructive testing (NDT) and laser cladding were chosen for test purpose. The results yielded by the proposed method were compared with those by other four classic methods widely used in the literatures, i.e., Otsu's method [11], Hou's method [13], KAPUR [15] and MET [18]. Quality of segmentation result is quantitatively evaluated by misclassification error (ME) measure [20], which regards image

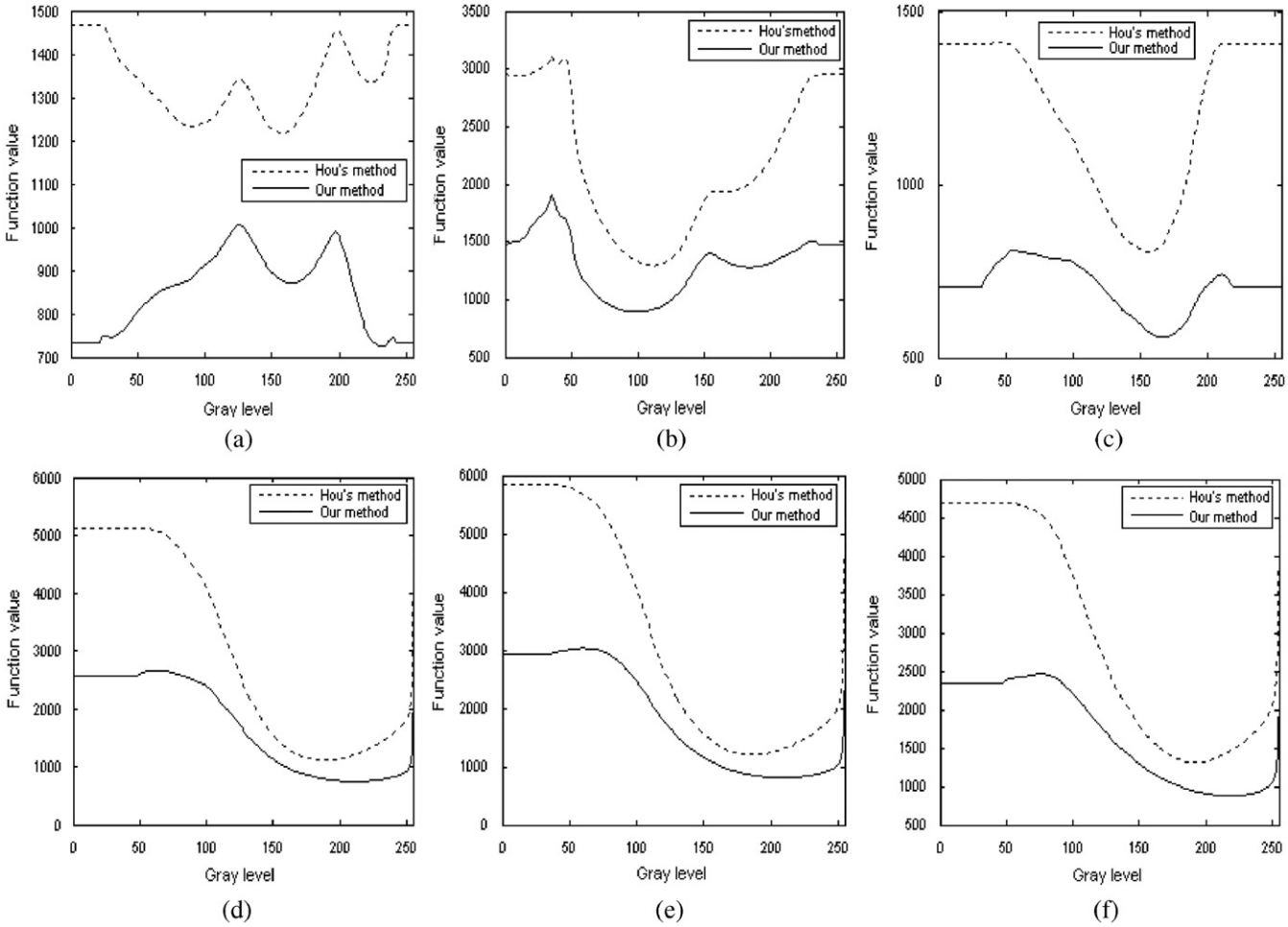

Fig. 3. Curves of two criteria for images: (a) GFRP, (b) PCB, (c) Material, (d) Laser1, (e) Laser2, (f) Laser3.

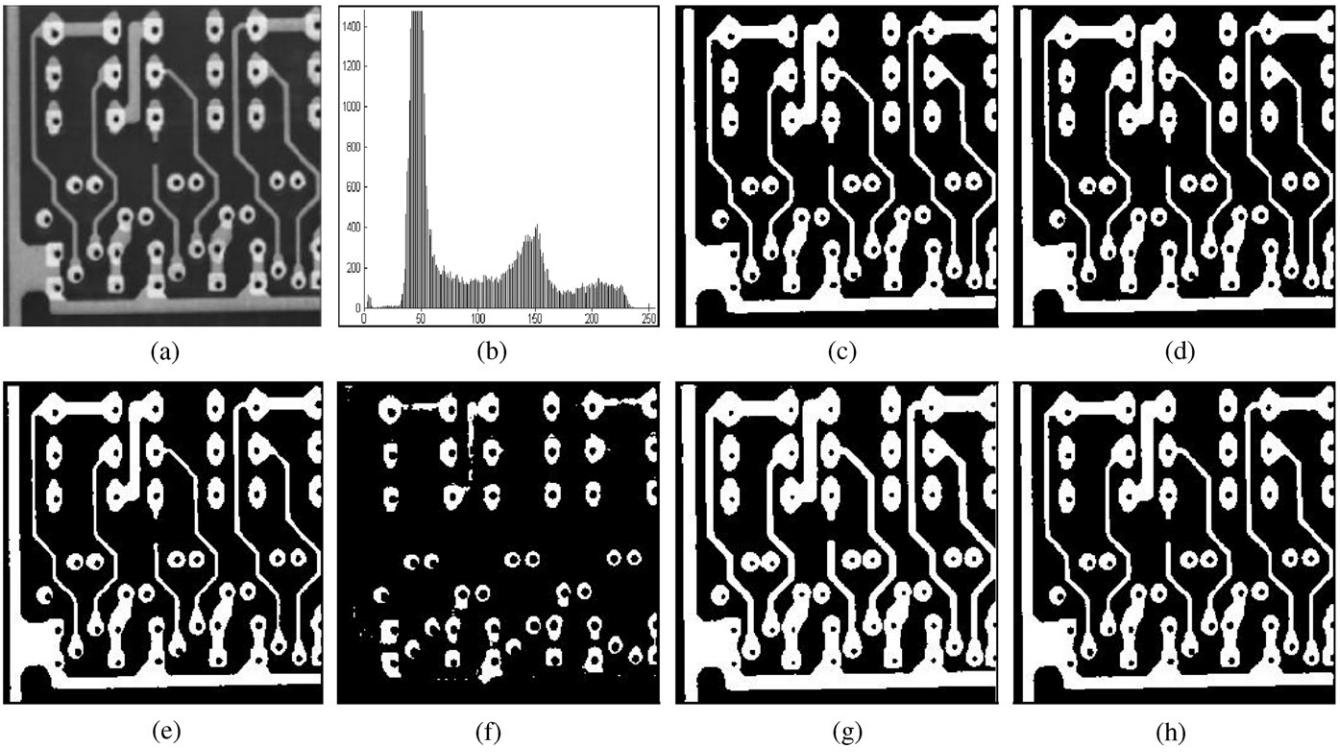

Fig. 4. Thresholding results of PCB image: (a) original, (b) histogram, (c) ground truth image, (d) Otsu's method ($t = 104$), (e) Hou's method ($t = 112$), (f) KAPUR ($t = 158$), (g) MET ($t = 64$), (h) the proposed method ($t = 99$).

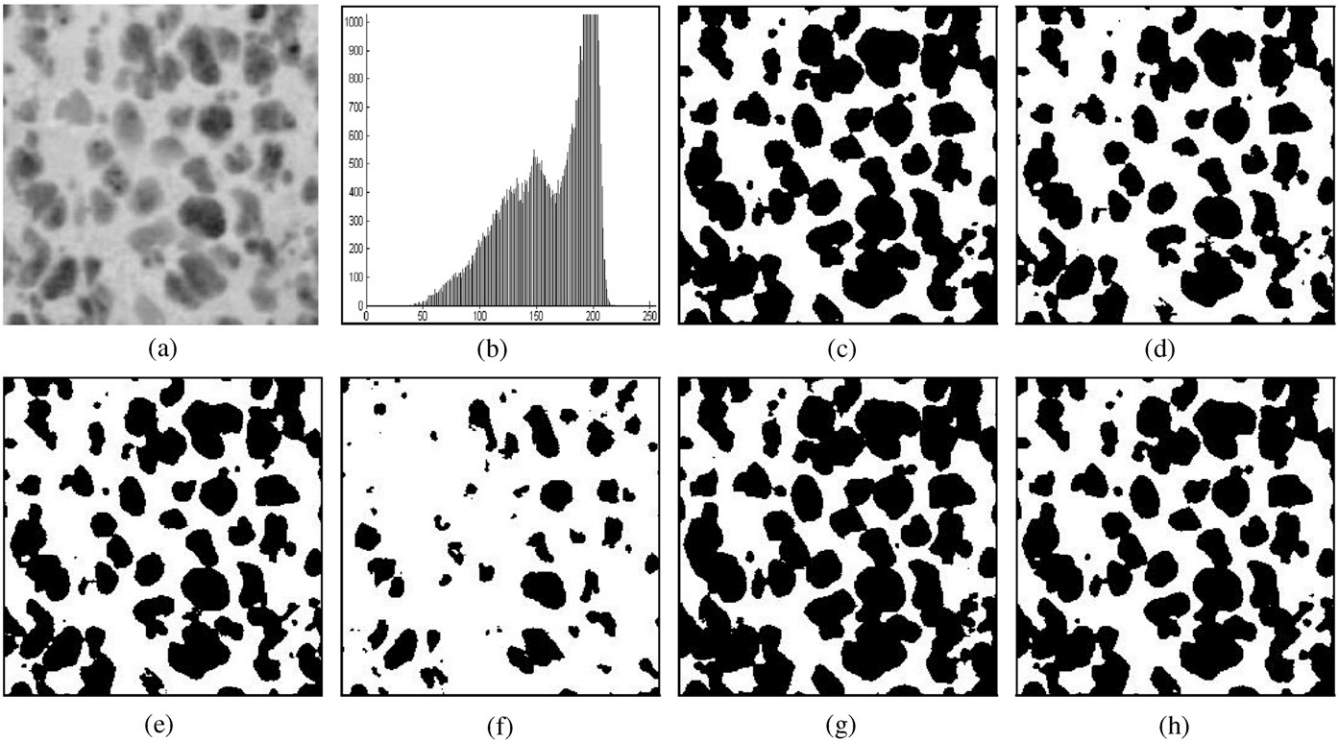

Fig. 5. Thresholding results of material image: (a) original, (b) histogram, (c) ground truth image, (d) Otsu's method ($t = 154$), (e) Hou's method ($t = 157$), (f) KAPUR ($t = 119$), (g) MET ($t = 177$), (h) the proposed method ($t = 167$).

segmentation as a pixel classification process. It reflects the percentage of background pixels incorrectly classified into foreground, and conversely, foreground pixels erroneously assigned to background. For a two-class segmentation, ME can be simply formulated as

$$\mathrm{ME} = 1 - \frac{|B_O \cap B_T| + |F_O \cap F_T|}{|B_O| + |F_O|}, \tag{18}$$

Table 2
Thresholds, numbers of misclassified pixels, values of ME, FPR and FNR, and running times obtained by using different methods for the laser cladding images.

Images	Thresholding methods				
	Otsu's method	Hou's method	KAPUR	MET	The proposed method
Laser1					
Threshold	175	189	100	253	211
Misclassified pixels	3763	2329	25972	2871	539
ME	0.057419	0.035538	0.3963	0.043808	0.0082245
FPR	0.085342	0.05282	0.58903	0	0.012224
FNR	0	0	0	0.13389	0
Running time (s)	0.344	2.531	0.047	0.203	3
Laser2					
Threshold	164	187	92	252	209
Misclassified pixels	3237	1618	19511	2565	299
ME	0.049393	0.024689	0.29771	0.039139	0.0045624
FPR	0.067087	0.033533	0.40436	0	0.0061968
FNR	0	0	0	0.14839	0
Running time (s)	0.235	2.578	0.031	0.141	2.937
Laser3					
Threshold	166	193	109	253	218
Misclassified pixels	5460	2428	18016	3329	296
ME	0.083313	0.037048	0.2749	0.050797	0.0045166
FPR	0.10599	0.047131	0.34972	0	0.0057458
FNR	0	0	0	0.23745	0
Running time (s)	0.203	2.406	0.032	0.093	2.86

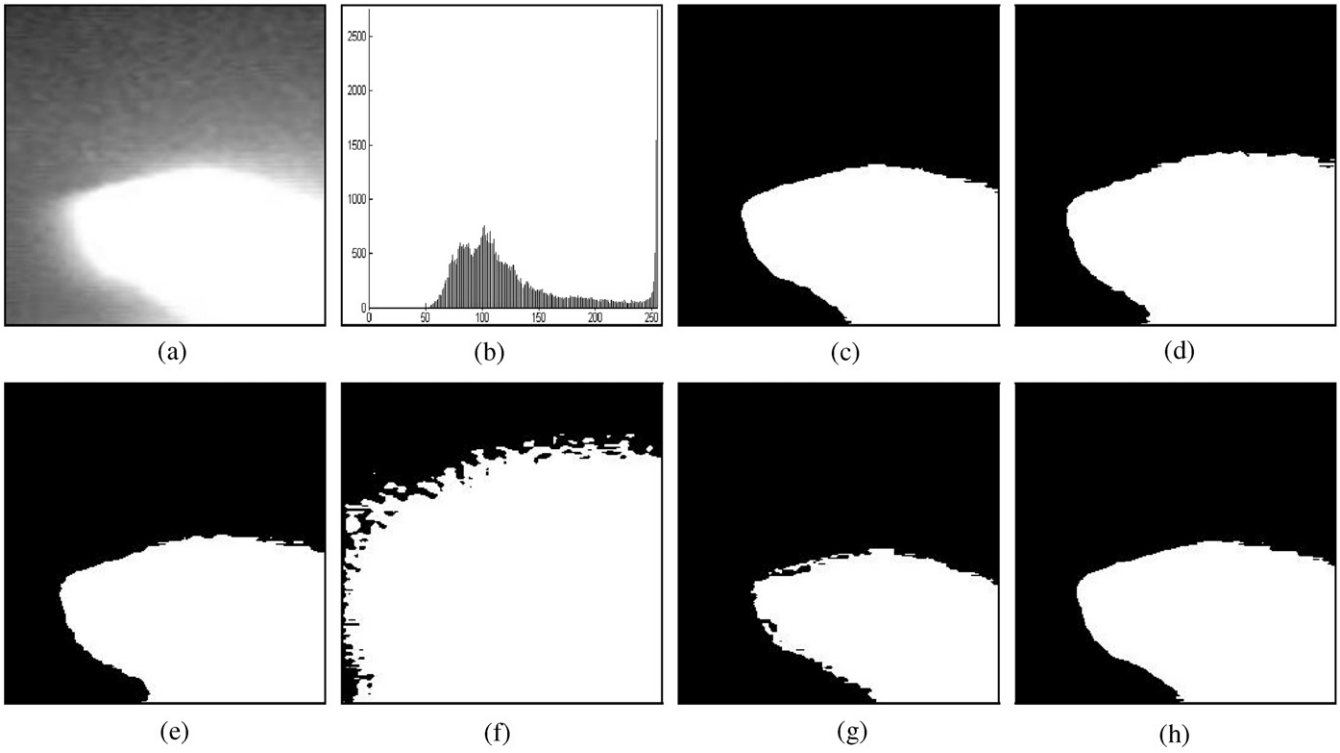

Fig. 6. Thresholding results of laser1 image: (a) original, (b) histogram, (c) ground truth image, (d) Otsu's method ($t = 175$), (e) Hou's method ($t = 189$), (f) KAPUR ($t = 100$), (g) MET ($t = 253$), (h) the proposed method ($t = 211$).

where B_O and F_O are the background and foreground of the ground truth image, B_T and F_T the background and foreground pixels in the thresholded image, and $|\cdot|$ cardinality of a set. The value of ME varies between 0 for a perfectly classified image and 1 for a totally erroneously classified one. A lower value of ME means better quality of corresponding thresholded image.

In order to provide more details about classification error, we introduce other two measures [21], i.e., false positive rate (FPR) and false negative rate (FNR). FPR is the rate of the number of background pixels misclassified into foreground to the total number of background pixels in the ground truth image. Similarly, FNR is the rate of the number of foreground pixels misclassified into background to the total number of foreground pixels in the ground truth. For a two-class segmentation, FPR and FNR can be respectively formulated as

$$\mathrm{FPR} = \frac{|B_O \cap F_T|}{|B_O|}, \tag{19}$$

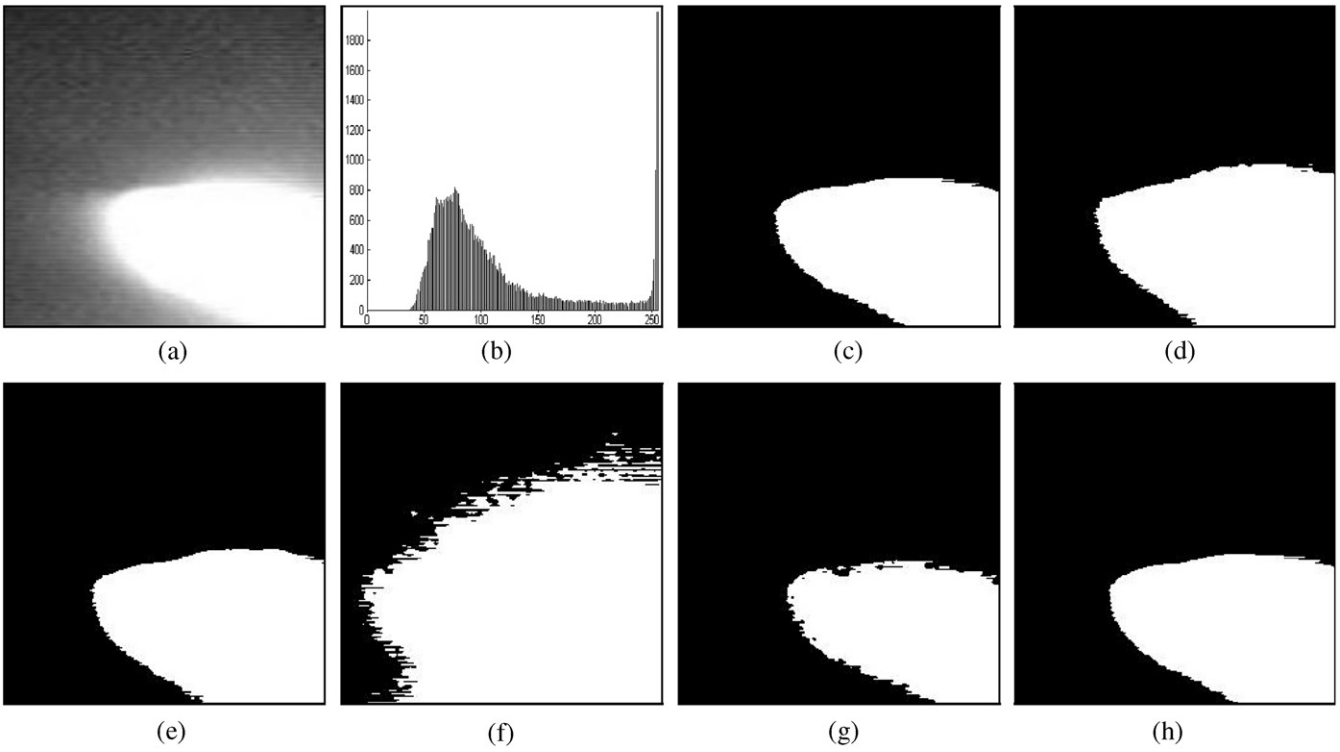

Fig. 7. Thresholding results of laser2 image: (a) original, (b) histogram, (c) ground truth image, (d) Otsu's method ($t = 164$), (e) Hou's method ($t = 187$), (f) KAPUR ($t = 92$), (g) MET ($t = 252$), (h) the proposed method ($t = 209$).

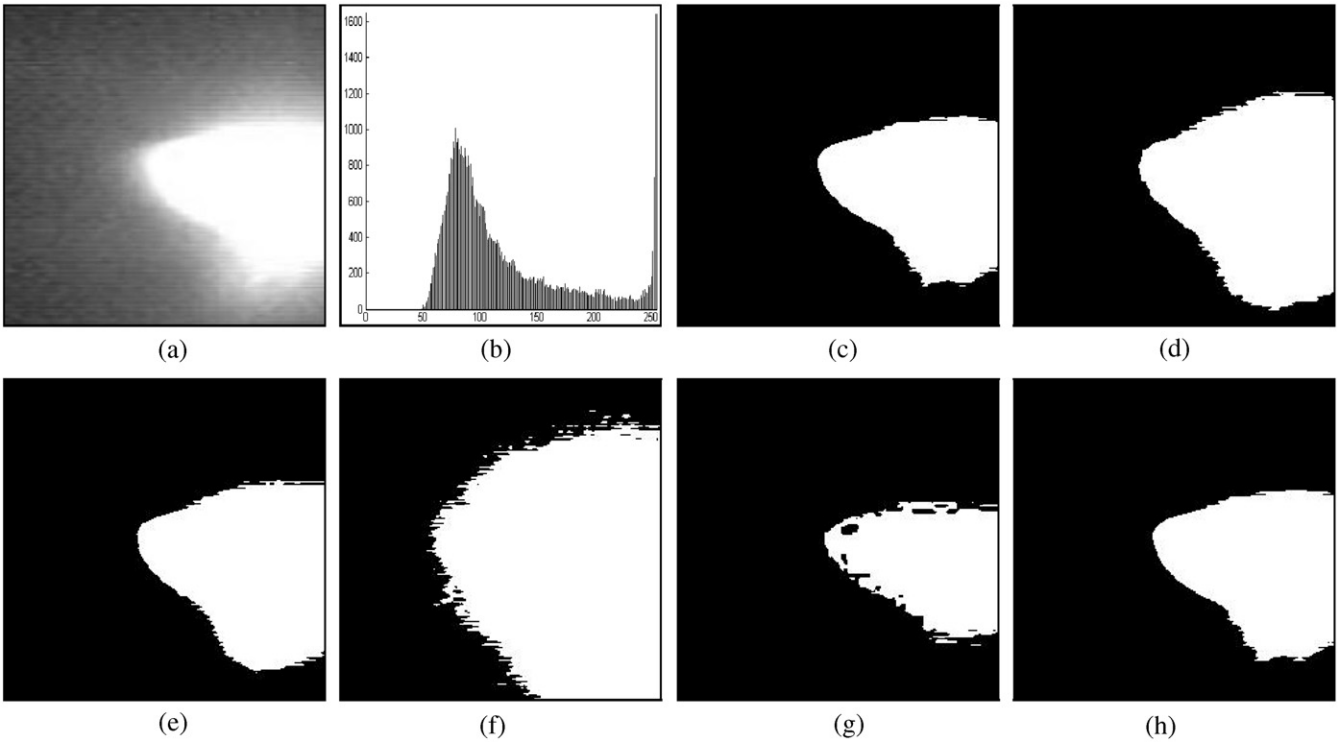

Fig. 8. Thresholding results of laser3 image: (a) original, (b) histogram, (c) ground truth image, (d) Otsu's method ($t = 166$), (e) Hou's method ($t = 193$), (f) KAPUR ($t = 109$), (g) MET ($t = 253$), (h) the proposed method ($t = 218$).

$$\mathrm{FNR} = \frac{|F_O \cap B_T|}{|F_O|}. \tag{20}$$

The values of FPR and FNR also vary between 0 and 1. FPR and FNR indicate over-segmentation and under-segmentation, respectively. High values of FPR and FNR correspond to serious over-segmentation and under-segmentation, respectively. In our practical calculations of FPR and FNR, we assume that foreground pixels have higher gray levels than background ones. In the proposed method, the parameter $\alpha = 0.5$. All experiments are performed on a

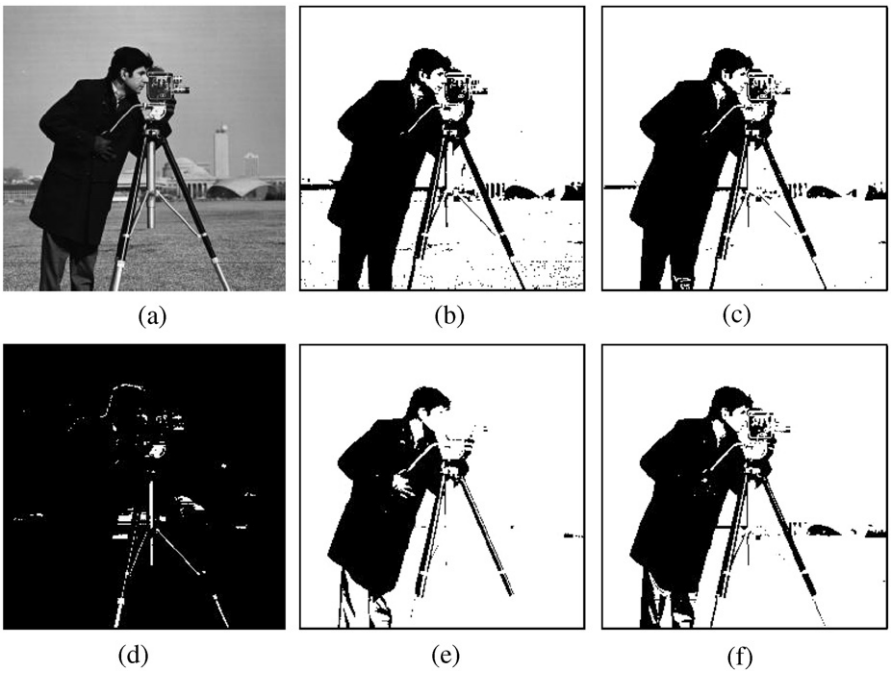

Fig. 9. Thresholding results of cameraman image: (a) original, (b) Otsu's method ($t = 88$), (c) Hou's method ($t = 67$), (d) KAPUR ($t = 192$), (e) MET ($t = 24$), (f) the proposed method ($t = 52$).

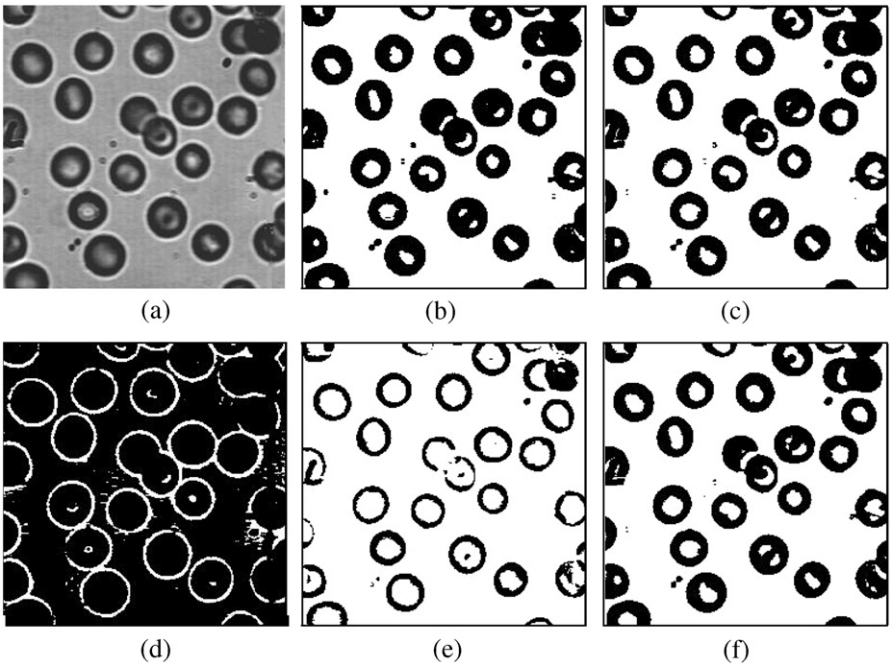

Fig. 10. Thresholding results of blood image: (a) original, (b) Otsu's method ($t = 111$), (c) Hou's method ($t = 98$), (d) KAPUR ($t = 174$), (e) MET ($t = 49$), (f) the proposed method ($t = 92$).

notebook PC with 2.13G Intel Core 2 Duo CPU and 3G RAM. All the images used in the experiments are of 256×256 pixels.

3.1. Experiments on NDT images

Two NDT images were first chosen and compared. They are a PCB and a light microscopy form of a material structure. NDT means to detect an object and quantify its possible defects without harmful effects on it by special equipments and methods. NDT is used in a broad variety of applications, such as aeronautics and astronautics, nuclear industry, chemistry and civil constructions.

The results in terms of thresholds, numbers of misclassified pixels, values of ME, FPR and FNR, and running times obtained by applying various methods to the images are listed in Table 1. The table shows that segmentation results yielded by our method have less misclassified pixels and lower ME values, that is, the new method obtains better results. This observation can further be judged by comparing what could be perceived in Figs. 4 and 5. From these figures, one can conclude that our segmentation results are closest to

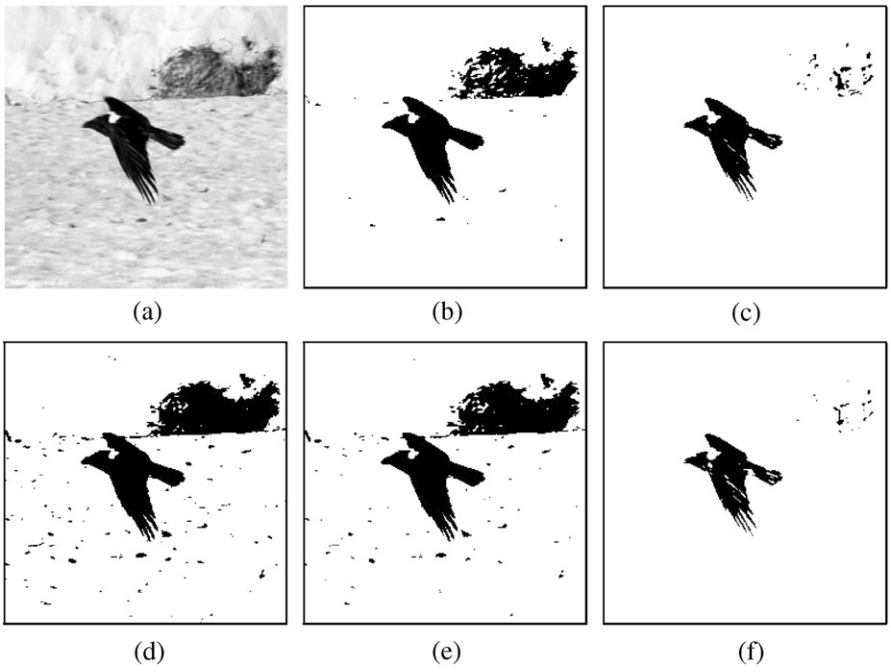

Fig. 11. Thresholding results of crow image: (a) original, (b) Otsu's method ($t = 142$), (c) Hou's method ($t = 56$), (d) KAPUR ($t = 182$), (e) MET ($t = 175$), (f) the proposed method ($t = 41$).

Table 3
ME values obtained by using the proposed method with different α.

Images	0.1	0.2	0.3	0.4	0.5	0.6	0.7	0.8	0.9	1
GFRP	0.03362	0.03362	0.03362	0.03362	0.00529	0.00357	0.00133	0.57547	0.58400	0.59236
PCB	0.32605	0.04938	0.02657	0.01524	0.00200	0.00609	0.01311	0.01999	0.02222	0.02675
Material	0.49641	0.49641	0.49641	0.00638	0.01892	0.03656	0.04868	0.06157	0.07466	0.08153
Laser1	0.02766	0.02017	0.01219	0.00180	0.00822	0.01843	0.02437	0.03005	0.03279	0.03554
Laser2	0.02725	0.02104	0.01260	0.00284	0.00456	0.01244	0.01697	0.02083	0.02281	0.02469
Laser3	0.03174	0.02287	0.01436	0.00604	0.00452	0.01317	0.02838	0.03192	0.03442	0.03705
Average ME	0.15712	0.10725	0.09929	0.01099	0.00725	0.01504	0.02214	0.12330	0.12848	0.13299

the ideal ones. Among the rest of methods, two classic statistical methods obtain similar results with under-segmentation. KAPUR exists serious under-segmentation, and conversely, MET exists over-segmentation. The judgment about over-segmentation and under-segmentation can be validated by FPR and FNR. In addition, Table 1 also shows that running time of our method is generally longer than those of other methods including two statistical ones, i.e., Otsu's and Hou's methods. But it is worth mentioning that running time of our method is usually less than 3 s for an image of 256×256 pixels. It basically meets real-time segmentation tasks. Although criterions of the three statistical methods are similar, we can observe from the table that Otsu's method is obviously faster than our method and Hou's method. This is because that we coded the latter two methods by Matlab 7.0, but Otsu's code comes from the inherent function named 'graythresh' of Matlab. Style of Otsu's code is different from those of our codes. The former better utilizes some inherent functions of Matlab to implement Otsu's method, which shortens its running time. Furthermore, Hou's method is slightly faster than our method. The reason is that our method needs extra time to compute variance discrepancy, as compared with Hou's method.

3.2. Experiments on laser cladding images

In this section, three laser cladding images were used for test purpose, namely Laser1, Laser2 and Laser3, respectively. Laser cladding by powder injection is an advanced material processing technology with applications in manufacturing, part repairing, metallic rapid prototyping and coating. A laser beam melts powder and a thin layer of the substrate to create a layer on the substrate. It is crucial to have a reliable feedback system for closed loop control over this process. Accurate segmentation of laser cladding images plays a pivotal role in the feedback system.

Laser cladding images have a common characteristic, that is, their object and background have obvious distinctive gray level changes, which results in large variance discrepancy of the object and background classes. Quantitative comparisons of segmentation results yielded by various methods are listed in Table 2, which shows that our results correspond to less misclassified pixels and lower ME values. In other words, the proposed method achieves better segmentation effect. Visual thresholded results are displayed in Figs. 6–8. From these figures, one can observe that our results are closest to the ground truth images.

3.3. Experiments on other images

In order to further compare the performance of various methods, two classic gray level images and a general real world image are chosen here. The first image is a cameraman of multimodal distribution, which consists of multiple parts, such as the man, white buildings, grassland and sky. For a two-class

segmentation problem, the man is our object, and the remainder is the background. Other two images are a blood cell and a crow flying in sky, respectively. Gray level changes of crow's body are small, and conversely, its background has obvious gray level changes. This causes large variance discrepancy of the object and background classes. The first two images have similar characteristic with the crow image.

Segmentation results obtained by applying various methods to the images are shown in Figs. 9–11. These images are of more complex structures than those in NDT and laser cladding, which are not suitable for quantitative measurement of segmentation quality. Quality of the results is only compared by visual perception. Figs. 9–11 show that our method achieves better visual effect, as it not only preserves more details of objects, but also contains less background noise. Among the reference methods, Otsu's and Hou's methods obtain similar results, but the latter contains less background noise. KAPUR yields worst results. MET exists under-segmentation for the first two images, and conversely, it exists over-segmentation for the last one.

3.4. Parameter

In the proposed method, there is only one parameter α, which is used to control weight of class variance sum and variance discrepancy in our new criterion. The smaller the α, the larger the weight of variance discrepancy. A series of experiments on images with different α have been carried out to find the reasonable value of α. Experimental results are listed in Table 3. The table shows that: (1) ME values of images usually vary from big to small, then from small back to big. This indicates that a too small or too big α will affect quality of segmentation results. When α is very small, our criterion will be mainly composed of variance discrepancy, which makes class variance sum be an implicit factor and neglects its effect to some extent. On the contrary, when α is very big, the criterion will degenerate to Hou's criterion, which neglects the effect of variance discrepancy. But it is worth mentioning that the advantage of our criterion is its comprehensive consideration for class variance sum and variance discrepancy. Each of them should be important for us. (2) Various images have different optimal value of α. However, we can also observe that the difference of ME values is small when α is between 0.4 and 0.6. In other words, our method is little affected by selection of α when it locates between 0.4 and 0.6. Therefore, as a general guide, the parameter α ranges between 0.4 and 0.6, a 0.5 is selected for the proposed method. The reason is that our method has lowest average ME value when α is 0.5.

4. Conclusions

Statistical thresholding method is a kind of common technique for image binarization. Two popular statistical methods, i.e., Otsu's and Hou's methods, choose class variance sum of some form as criterions for threshold selection. Both methods only take variance sum of the object and background classes into account, but neglect their variance discrepancy. Thus they fail to obtain satisfactory results when segmenting those images with large variance discrepancy, such as NDT images and laser cladding images. In order to eliminate the above limitation, a new statistical criterion is proposed in this paper, which considers class variance sum and variance discrepancy simultaneously. The proposed method can be regarded as a generalized version of Hou's method, because when α is one, their criterions are the same. Experimental results on a variety of real world images demonstrate the effectiveness of the proposed method.

Acknowledgments

This work is supported by National Natural Science Foundation of China (Grant nos. 60472061, 60632050, 90820004), National 863 Project (Grant nos. 2006AA04Z238, 2006AA01Z119), Technology Project of provincial university of Fujian Province (2008F5045), Project of the Technology Department of Fujian Province (2007F5083) and Technology Startup Project of Minjiang University (YKQ07001).

References

[1] Yuksel ME. Edge detection in noisy images by neuro-fuzzy processing. AEU Int J Electron Commun 2007;61:82–9.
[2] Kwon SH. Threshold selection based on cluster analysis. Pattern Recognition Lett 2004;25:1045–50.
[3] Wang S, Chung F, Xiong F. A novel image thresholding method based on parzen window estimate. Pattern Recognition 2008;41:117–29.
[4] Demirci R. Rule-based automatic segmentation of color images. AEÜ Int J Electron Commun 2006;60:435–42.
[5] Sund T, Eilertsen K. An algorithm for fast adaptive binarization with applications in radiotherapy imaging. IEEE Trans Med Imaging 2003;22:22–8.
[6] Solihin Y, Leedham CG. Integral ratio: a new class of global thresholding techniques for handwriting images. IEEE Trans Pattern Anal Mach Intell 1999;21:761–8.
[7] Bhanu B. Automatic target recognition: state of the art survey. IEEE Trans Aerosp Electron Syst 1986;22:364–79.
[8] Bruzzone L, Prieto DF. Automatic analysis of the difference image for unsupervised change detection. IEEE Trans Geosci Remote Sensing 2000;38:1171–82.
[9] Tsai WH. Moment-preserving thresholding: a new approach. Comput Vis Graph Image Process 1985;29:377–93.
[10] Bazi Y, Bruzzone L, Melgani F. Image thresholding based on the EM algorithm and the generalized Gaussian distribution. Pattern Recognition 2007; 40:619–34.
[11] Otsu N. A threshold selection method from gray-level histograms. IEEE Trans Syst Man Cybern 1979;9:62–6.
[12] Sahoo PK, Soltani S, Wong AKC. A survey of thresholding techniques. Comput Vis Graph Image Process 1988;41:233–60.
[13] Hou Z, Hu Q, Nowinski WL. On minimum variance thresholding. Pattern Recognition Lett 2006;27:1732–43.
[14] Pun T. A new method for grey-level picture thresholding using the entropy of the histogram. Signal Process 1980;2:223–37.
[15] Kapur JN, Sahoo PK, Wong AKC. A new method for grey-level picture thresholding using the entropy of the histogram. Comput Vis Graph Image Process 1985;29:273–85.
[16] Liu D, Jiang ZH, Feng HQ. A novel fuzzy classification entropy approach to image thresholding. Pattern Recognition Lett 2006;27:1968–75.
[17] Saha PK, Udupa JK. Optimum image thresholding via class uncertainty and region homogeneity. IEEE Trans Pattern Anal Mach Intell 2001;23:689–706.
[18] Kittler J, Illingworth J. Minimum error thresholding. Pattern Recognition 1986;19:41–7.
[19] Sezgin M, Sankur B. Survey over image thresholding techniques and quantitative performance evaluation. J Electron Imaging 2004;13:146–65.
[20] Yasnoff WA, Mui JK, Bacus JW. Error measures for scene segmentation. Pattern Recognition 1977;9:217–31.
[21] Hu Q, Hou Z, Nowinski WL. Supervised range-constrained thresholding. IEEE Trans Image Process 2006;15:228–40.

Zuoyong Li received the B.S. degree in computer science and technology from Fuzhou University in 2002. He got his M.S. degree in computer science and technology from Fuzhou University in 2006. Now, he is a Ph.D. candidate in Nanjing University of Science and Technology and a lecturer in the department of computer science of Minjiang University. His research interests include image segmentation and pattern recognition.

Chuancai Liu is a full professor in the school of computer science and technology of Nanjing University of Science and Technology, China. He obtained his Ph.D. degree from the China Ship Scientific Research Center in 1997. His research interests include AI, pattern recognition and computer vision. He has published about 50 papers in international/national journals.

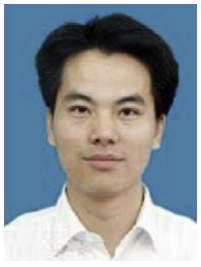

Guanghai Liu is currently an associate professor in the department of computer science and information technology of Guangxi Normal University, China. He received his Ph.D. degree from the school of computer science and technology at Nanjing University of Science and Technology in 2009. His current research interests include image processing, pattern recognition and artificial intelligence. He has published some papers in international/national journals.

Yong Cheng received the M.S. degree in computer science and technology from Nanjing University of Information Science and Technology in 2004. He is now a Ph.D. candidate in Nanjing University of Science and Technology, China. His research interests include image processing and pattern recognition.

Xibei Yang received the B.S. degree in computer science and technology from the Xuzhou Normal University in 2002. He received the M.S. degree in computer applications from Jiangsu University of Science and Technology in 2006. Currently, he is a Ph.D. candidate in Nanjing University of Science and Technology, China. His research interests include knowledge discovery and rough set theory.

Cairong Zhao was born in Jiangxi, China, in 1981. He received the B.S. degree in electronics and information scientific technology from Jilin University, China, in 2003 and M.S. degree from Changchun Institute of Optics, Fine Mechanics and Physics, Chinese Academy of Sciences, in 2006, respectively. He is currently pursuing the Ph.D. degree in the department of computer science from Nanjing University of Science and Technology. His research interests include face recognition, pattern classification, neural networks and vision attention.